Semiconducting Pop-Up Bolometers for Far-Infrared and Submillimeter Astronomy

S. Harvey Moseley, Jr.[1], C. Darren Dowell[2], Christine Allen[1] & Thomas G. Phillips[2]

Abstract.

Large format background-limited far infrared and submillimeter detector arrays are essential to enable the scientific exploitation of these important spectral bands. Much of the luminosity of the early universe is emitted in the rest frame far-infrared; we observe much of it at far infrared and submillimeter wavelengths. The success of the first generation of far infrared and submillimeter cameras provides a powerful motivation to extend these capabilities in a new generation of instruments. We describe the development of filled two-dimensional arrays of far-infrared detectors for such instruments. Such arrays make the best possible use of the valuable real estate found in the focal planes of submillimeter telescopes.

1. Introduction

Observations of the Cosmic Microwave Background by COBE and its successor ground based and balloon-borne experiments trace the distribution of gravitational potential in the universe at the time of decoupling of the CMB from matter at a redshift of about 1000. These measurements reveal a very smooth universe, with RMS gravitational potential fluctuations of only $\sim 10^{-5}$ of the mean at that time. During the next few billion years, the universe develops into the highly structured system seen in the Hubble Deep Field. A primary goal of astrophysics is to provide the observational basis to understand the processes leading to this dramatic transformation in the epoch of galaxy formation. The first deep surveys in the submillimeter by SCUBA (Hughes et al., 1998) have shown that the optical and near infrared measurements tell only a partial story of the development in this critical epoch of galaxy formation. Much of the luminosity of galaxies in this phase of the universe is emitted in the far infrared. Therefore, to understand the history of nucleosynthesis and structure formation in the universe, high sensitivity far infrared and submillimeter observations are essential.

To make full use of the opportunities provided by this submillimeter window on the early universe, space missions are required. ESA's Far Infrared Space Telescope (FIRST) will further refine number counts in this epoch of formation.

---

[1]NASA Goddard Space Flight Center, Mail Stop 685.0, Greenbelt, MD 20771. Email: moseley@stars.gsfc.nasa.gov,callen@pop500.gsfc.nasa.gov

[2]California Institute of Technology, Mail Code 320-47, Pasadena, CA 91125. Email: cdd@submm.caltech.edu, phillips@submm.caltech.edu

Ultimately, a cryogenic space mission with sufficient angular resolution to avoid spatial confusion is required. Studies to define such a mission are now underway (e.g. Mather et al., 1999).

To make the most rapid progress in addressing this problem of initial structure formation, we must make the best possible use of existing facilities while developing the technologies which will enable the future space missions. One of the most effective ways to extend the capabilities of existing telescopes is to improve their detector systems. Most detector systems presently work with high optical efficiency and are background limited, so significant improvements in individual detector performance are not possible. However, the size of the detector arrays can be significantly increased to allow use of the full focal plane provided by the telescope facility.

We describe one such effort to develop large format arrays. We are developing filled two dimensional arrays of detectors which instantaneously spatially Nyquist sample the focal plane of the telescope. All the detectors in the array share a common set of cryogenic beam forming optics which limit the $A\Omega$ on each detector to $\lambda^2/4$. With the throughput thus limited, the system has performance which is similar to that of a diffraction limited CCD in the visible; the beam efficiency of each pixel is smaller than that of an efficient single mode feedhorn (with a diameter of $2f\lambda$ in the focal plane) , but because of the lower background and noise due to the smaller $A\Omega$ and the requirement for multiple samples to provide full sampling in the case of the feedhorn, the signal to noise ratios in the two systems for a source of unknown position are identical. Thus the observing speed of a filled array is improved over an array of coherent feeds of the same total size approximately by the ratio of their total $A\Omega s$, resulting in a factor of $\sim$3.4 speed increase of the filled array over a hexagonal close-packed array of $2f\lambda$ coherent feeds for fixed focal plane area.

There are practical difficulties in the production of such filled arrays of thermal detectors. First, the focal plane must be fully sampled with a high filling factor. While achieving this high filling factor, the thermal conductance between the detector and its heat sink must be tailored to its proper low value. Finally, the signal from each detector must be routed to its cryogenic amplifier and then to the outside world for digitization and sampling, while providing for intimate coupling between the detector and its cryogenic preamp. We describe the architecture we have developed for achieving these requirements. Our devices, called Pop-up Detectors (PUDs) meet all these requirements using micromachined single crystal Si detector elements. In this paper, we describe the PUD arrays being developed for the SHARC II camera for the CSO and the HAWC instrument for SOFIA. These devices use ion-implanted Si semiconductor thermometers and JFET amplifiers. We describe the geometry of the detector and detector package, and identify the critical components required for its fabrication.

The ultimate goal of this development program is to produce large arrays of detectors with multiplexed readouts. Progress on the production of such an array using superconducting transition edge thermometers (TESs) (Irwin, 1995) and SQUID multiplexers (Chervenak et al., 1999) is described by Benford et al. (1999) in these proceedings.

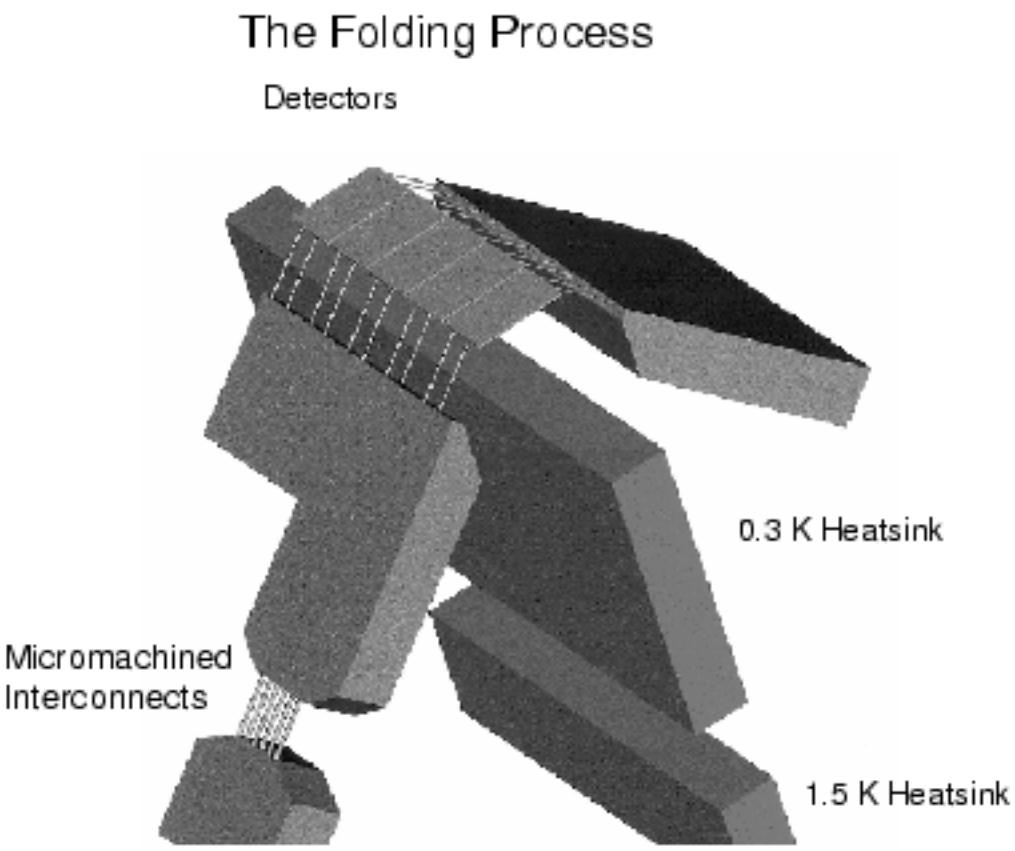

Figure 1. PUD being folded onto the heat sinks. The devices are made by a planar process and then folded into stackable linear arrays.

2. Array Concept

The Pop-up detector array is produced by folding a linear array of detectors about the long axis of the array. (Figure 1). This results in a linear array in which the electrical connections and heat sink for the detector are hidden behind the line of pixels as seen from the photon input side. These linear arrays can be close packed to produce a two dimensional array, while still providing easy electrical and thermal connection to detectors over the entire array. We will demonstrate that we can achieve the required optical, thermal, and electrical parameters required for background limited operation of Pop-up arrays.

2.1. Optical coupling

A high performance detector system must efficiently absorb light arising from the solid angle subtended by the telescope while rejecting any background arising outside it. In the Pop-up detector design, the beams for all detectors in the focal plane are formed by a common cryogenic optical system of lenses or mirrors and stops. The efficient absorption of the incident light is accomplished by using a resistive film on the detector. If very broad band operation is required, a

free space matching film (with no backshort) can provide ~50 % absorption efficiency over all wavelengths, limited only by the change in optical properties of Si in the near infrared and by the transmission of the essentially capacitive grid of detectors at very long wavelengths. For applications where the fractional wavelength range is less than ~4, higher performance can be achieved by using a $1/4\lambda$ backshort. Near band center, efficiencies of over 90% are achieved, and 60% is possible over the 4 to 1 wavelength range. For SHARC II, where only the 350 and $450\mu m$ windows will be used, the resonant absorber offers significant performance advantages, allowing us to achieve over 90% absorption over the 350 μm band.

One concern in the design of the pixel is any possible effect on the optical performance of the detector due to the implanted thermometer itself. The optimization of the detector performance requires the thermometer to cover the entire pixel to limit the magnitude of the $1/f$ noise from the resistance fluctuations in the thermometer (Han et al. 1998). In order to assess the optical effect of the thermometer, the reflection of an implanted Si sample was measured at 4.2 K. Its effective surface impedance was found to range between 1100 and 1500 Ω/square over the 50 to 500 μm spectral range. This resistance appears in parallel with that of the absorbing film (with a small phase shift because of the $1\mu m$ detector thickness), and thus must be included in the absorber design.

2.2. Electrical Interconnections and Thermal Isolation

To achieve background limited performance, submillimeter thermal detectors must be cooled to temperatures below ~0.3 K. The amplifiers which offer the best performance for use with semiconducting detectors are JFETs, which operate near 100 K, so close coupling of the detector and amplifier requires careful thermal engineering. Typically, electrical connections between components of different temperatures have been accomplished using cables of resistance wire, such as manganin, to simultaneously provide electrical connections and low thermal conductance. As we move to much larger format detectors, such an approach becomes less practical. We have developed micromachined electrical interconnections to solve this problem. In these devices thin micromachined conductors bridge the thermal interface. Electrical connection on each side is made by conventional wire bonds. This results in a very compact set of electrical connections well suited to the requirements of our two dimensional arrays. These electrical interconnections have been qualified for and are being used in the detector assemblies for the Infrared Array Camera (IRAC) to fly on SIRTF.

The JFET amplifiers must operate at ~100 K, but should be very close to the detectors to avoid microphonics due to the modulation of the input capacitance of the system by ambient vibrations. The FETs must be well isolated thermally so they achieve the required operating temperature of 100 K with only the dissipation from their minimum drain current. In our design, the mechanical support is achieved using tubular G-10 elements, and electrical connection with micromachined bridges. The most difficult challenge is the protection of the detectors from the thermal radiation of the JFETs. The JFETs are enclosed in a metal box, but the input and output electrical connectors provide significant opportunity for leaks. This problem has been solved in other applications by using multiple shields as required.

2.3. Load Resistors

The load resistors are thin film SiCr devices. A sample resistor has been tested for noise and has been shown to have no significant excess above Johnson noise while operated at the required current down to a frequency of 0.1 Hz. For design convenience, we have chosen to operate the load resistors on the ^{4}He bath. In order that this higher temperature load resistor not dominate the noise of the detector, its resistance must be larger than that of the detector at least by the ratio of their temperatures. A mask for a custom array of 32 400 MΩ resistors has been produced, and the resistors will be produced by Mini Systems, Inc.

2.4. Structural System

We have chosen Kevlar as the structural support material for the detectors because it has among the highest ratios of strength and stiffness to thermal conductivity in the 1.5 K region of any material. We have designed the detector support as a tensile kinematic structure, with six rigid Kevlar constraints, each with its own spring-loaded Kevlar tensioning fiber. In such a system, all straps can be tensioned independently. The tension in each element is known, and the resonant frequencies of the system are independent of the tension of the supports in the linear range. This results is a stable and predictable mechanical system, which has been demonstrated by test in the case of the detector mounts for the IRAC instrument. High resonant frequencies are achieved with low thermal conductance. One concern is the long-term creep of the Kevlar. After tensioning, the kevlar continues to creep in a logarithmic fashion. In this design, the tensioner will assure that the constraints remain in tension, but the dimensional changes could stress the electrical interconnects beyond acceptable limits. Since most of the creep occurs soon after tensioning, we will address this problem by pre-relaxing the support system and waiting for a relaxation time before installing the detectors in the structure.

3. Bolometers for SHARC II

We now discuss the practical design considerations of a pop-up bolometer array for the SHARC II instrument (Dowell, Moseley, & Phillips 1999), the successor to SHARC (Wang et al. 1996). Each pixel in the SHARC II array will have one thermistor at ∼0.5 K, one 400 MΩ load resistor at 1.5 K, and one JFET at ∼120 K. All of the components, thermal isolation, and radiation shielding for a 6×32 array will be packaged in a ceramic housing (Figure 2).

For SHARC II, we are constructing an AC-biased readout (Wilbanks et al. 1990) with an optical signal band of approximately 0.1 to 50 Hz. It is necessary to have good low frequency stability of the bolometer signal so that sensitivity to large spatial wavelengths is obtained as the array is scanned over the sky. Low frequency noise from the amplifier is removed by AC biasing; however, low frequency noise in the bolometer and load resistors is not.

The background conditions have been calculated for SHARC II based on the instrument description of Dowell et al. (1999) and assuming reasonable weather ($\tau_{350\mu m} \sim 1$). The bolometer design restrictions are summarized in Table 1. We require that the detector noise increase the total system noise by less than 10%.

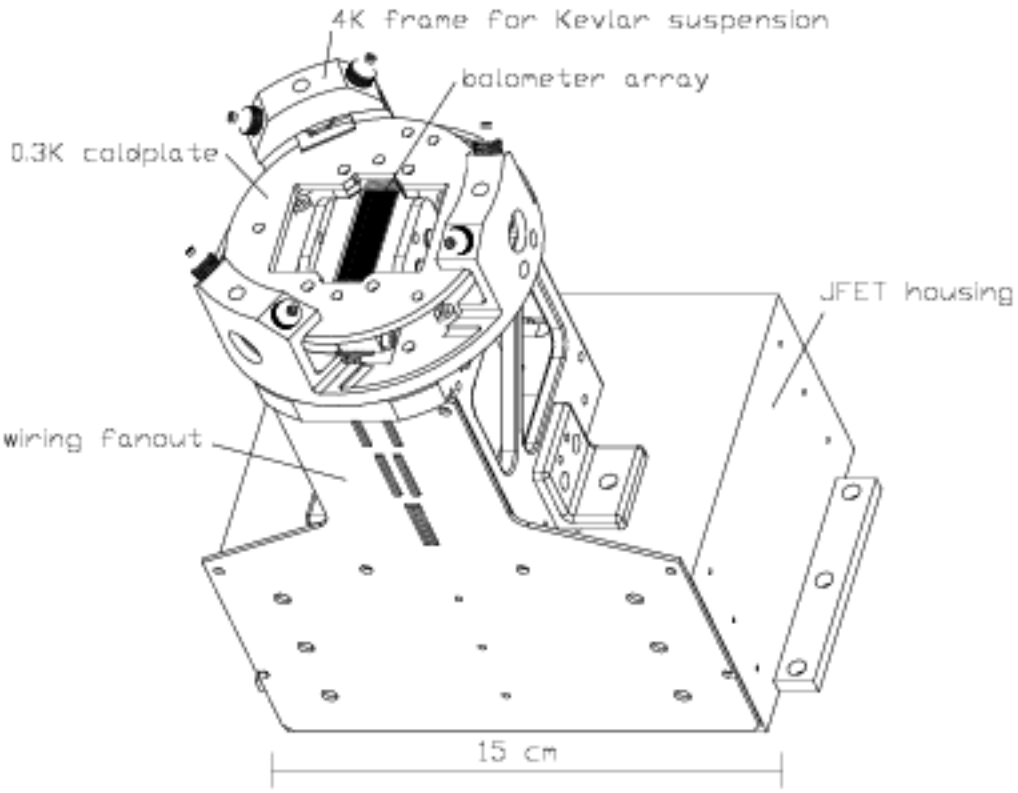

Figure 2. Housing designed to contain a 12×32 pop-up array, load resistors, and JFET amplifiers. The chief construction material is ceramic (alumina), chosen to match the low coefficient of thermal expansion of silicon. The SHARC II array will be partially populated, probably at the level of 6×32.

The resistance of the doped silicon thermistors is modeled well by the variable range hopping mechanism, where:

$$R = R_0 \exp(\sqrt{\frac{T_0}{T}}). \tag{1}$$

The dependence of T_0 on doping density is extreme, while the dependence of R_0 is weak (Zhang et al. 1993).

The temperature dependence of the thermal conductance in the silicon links is:

$$G = G_0 T^3 \tag{2}$$

We searched G_0, T_0, R_0 parameter space for a detector solution for SHARC II. Calculations of the NEP were based on the formulae of Mather (1982) and the 1/f thermistor noise predictions of Han et al. (1998). The proposed electrical and thermal design is given in Table 2. The 1/f noise is minimized by implanting the thermometer over the full area of the pixel. The values of R_0 and T_0 were chosen to be appropriate for a square thermistor (Zhang et al. 1993). Although

Table 1. SHARC II Bolometer Design Constraints

Operating temperature	0.32 K
Background power (Q)	75 pW
NEP_{elec}(sky)	4.4×10^{-16} W $Hz^{-1/2}$
NEP_{elec}(detector)	$\leq 2.0\times10^{-16}$ W $Hz^{-1/2}$
e_n(amplifier, 50 Hz)	6 nV $Hz^{-1/2}$
R_{load}	400 MΩ at 2.0 K
Signal bandwidth	f = 0.1 to 50 Hz

slightly better NEP's could be obtained with higher resistance, we restricted the resistance to <10 MΩ so that parasitic capacitance will not produce long duration glitches at the transition of the square wave bias (Wilbanks et al. 1990). We also raised G_0 somewhat from the optimum to lessen the dependence of responsivity on background power. The required values are easily accessible using convenient link geometries.

Table 2. SHARC II Bolometer Design

Parameter	Target	Acceptable Range	Units
R_0	1430	400-2000	Ω
T_0	40	31-43	K
G_0	8.0	1.5-9.5	nW K^{-4}
implant area	1		mm^2
time constant	1.5	less than 10	ms

The operating conditions and NEP of the SHARC II bolometers are given in Table 3. The bolometer warms up considerably above the heat sink due to the low thermal conductance, reducing the 1/f noise to an acceptable level (Han et al. 1998). The cost of the low thermal conductance is a large dependence of the responsivity S on the background power Q: (dS/dQ)/(S/Q) = -0.7. In SHARC, for comparison, the dependence was (dS/dQ)/(S/Q) = -0.4. This effect will be removed from the data by continuous monitoring of the bolometer total resistance, which varies inversely with background power in the case of stable bias voltage and stable base temperature.

To determine the required accuracy of the bolometer fabrication, we considered the range for each parameter separately for which we achieve our goal of NEP_{elec}(detector) $\leq 2.0\times10^{-16}$ W $Hz^{-1/2}$. This range has also been included in Table 2.

4. Summary

We have developed a design and component technologies for producing close-packed two dimensional arrays of thermal detectors. Such devices promise to extend the capabilities of ground based and airborne telescopes in the important submillimer spectral band. Two systems are being developed to use the pop-up detectors with semiconductor thermometers, the SHARC II instrument for the CSO, and the HAWC instrument for SOFIA. Similar detectors using superconducting thermometers and a SQUID multiplexer are being developed for the

Table 3. Calculated Bolometer Characteristics

Parameter	Value	Units
V(bias)	820	mV
V(bolometer)	20	mV
I	2.0	nA
R	10.0	MΩ
Z	5.1	MΩ
T	0.51	K
G	1.1	nW K^{-1}
S	1.2	10^8 V/W
NEP_{elec} (phonon)	0.89	10^{-16} W $Hz^{-1/2}$
NEP_{elec} (bol. Johnson)	1.03	10^{-16} W $Hz^{-1/2}$
NEP_{elec} (bol. 1/f, 0.1 Hz)	1.10	10^{-16} W $Hz^{-1/2}$
NEP_{elec} (load Johnson)	0.22	10^{-16} W $Hz^{-1/2}$
NEP_{elec} (amplifier)	0.50	10^{-16} W $Hz^{-1/2}$
NEP_{elec} (detector total)	1.84	10^{-16} W $Hz^{-1/2}$
e_n	22	nV $Hz^{-1/2}$

SPIRE instrument on FIRST (Benford et al. 1999). These systems all combine background-limited performance with simultaneous Nyquist sampling of the focal plane. Such detectors can significantly enhance the capabilities of existing facilities while motivating the development of more powerful space observatories.

References

Benford, D. J., et al. 1999, in Imaging at Radio through Submillimeter Wavelengths, ed. J. Mangum & S. Radford, ASP Conf. Ser.

Chervenak, J. A. , Irwin, K. D. , Grossman, E. N., Martinis, J. M., Reintsema, C. D., & Huber, M. E. 1999, Appl. Phys. Lett., 74, 4043

Dowell, C. D., Moseley, S. H., Jr., & Phillips, T.G. 1999, in Imaging at Radio through Submillimeter Wavelengths, ed. J. Mangum & S. Radford, ASP Conf. Ser.

Han, S.-I., et al. 1998, in EUV, X-Ray, and Gamma-Ray Instrumentation for Astronomy IX, ed. O. Siegmund & M. Gummin, Proc. SPIE 3445

Hughes, D. H., et al., 1998, Nature, 394, 241.

Irwin, K. D. 1995, App. Phys. Lett. 66, 1998

Mather, J. C. 1982, Appl.Optics, 21, 1125

Mather, J. C., et al. 1999, Astro-ph 9812454

Wang, N., et al. 1996, Appl.Optics, 35, 6629

Wilbanks, T., Devlin, M., Lange, A. E., Sato, S., Beeman, J. W., & Haller, E. E. 1990, IEEE Trans. Nuclear Sci., 37, 566

Zhang, J., Cui, W., Juda, M., McCammon, D., Kelley, R. L., Moseley, S. H., Stahle, C. K., & Szymkowiak, A. E. Phys.Rev.B, 48, 2312

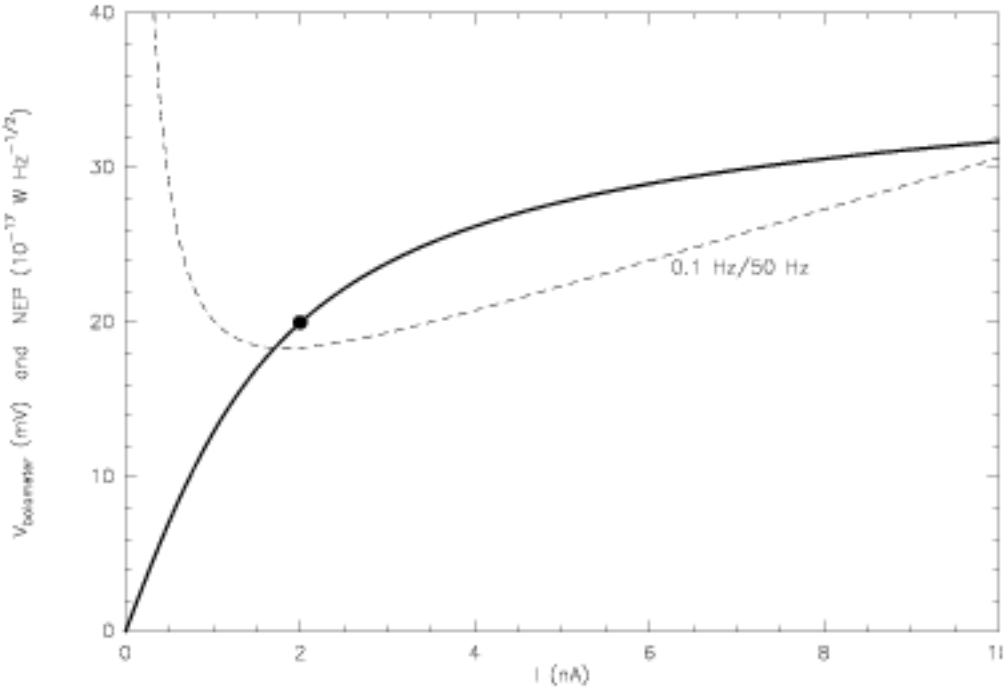

Figure 3. Simulated IV curve for bolometer optimized for SHARC II. The optimum operating point for AC biasing at 50 Hz (source modulation at 0.1 Hz) is shown with a dot. Also shown is the relation of detector NEP to the operating current (dashed line).